Proceedings World Geothermal Congress 2020+1
Reykjavik, Iceland, April - October 2021

How the Spatial Continuity of Permeability Affects Hydrothermal Convection: A Study Using Entropy Production

Jan Niederau*[1,4], Florian Wellmann[2], Nele Börsing[3]

[1] Institute for Applied Geophysics and Geothermal Energy, E.ON Energy Research Center, RWTH-Aachen University, Germany
now at: Geothermal Energy and Geofluids Group, Department of Earth Sciences, ETH Zürich, Switzerland

[2] Computational Geoscience and Reservoir Engineering, RWTH Aachen University, Germany

[3] Institute of Geophysics, Department of Earth Sciences, ETH Zürich, Switzerland

[4] Jülich-Aachen Research Alliance (JARA-HPC), RWTH Aachen University, Germany

E-mail: jan.niederau@erdw.ethz.ch

Keywords: Hydrothermal Convection, Entropy Production, Heterogeneous Permeability, Perth Basin, Spatial Continuity

ABSTRACT

With active convection in a reservoir, regions of upflow in convective systems can increase the geothermal energy potential of said reservoir; on the other hand, convection introduces uncertainty, because it is difficult to locate these regions of upflow. Several predictive criteria, such as the Rayleigh number, exist to estimate whether convection might occur under certain conditions. Once a convection system is established, diagnostic measures are needed for describing the convection pattern, e.g. the likely number of upwelling regions. We use the thermodynamic measure called entropy production to describe the influence of spatially heterogeneous permeability on a hydrothermal convection pattern in a hot sedimentary aquifer in the Perth Basin, Australia. To this end, we analyze the entropy production in multiple ensembles in a Monte Carlo study. Each ensemble contains several hundred realizations of spatially heterogeneous permeability. By observing the measure of entropy production, we see that the convection patterns in our models drastically change with the introduction and increase of a finite correlation length in permeability. An initial decrease of the average entropy production number with increasing lateral correlation length indicates that less ensemble members show convection. When neglecting the purely conductive ensembles in our analysis, no change in the convection pattern is seen for lateral correlation lengths larger 2000 m. Besides model dimensions, our results show that also the spatial anisotropy of important flow-parameters, such as permeability, is important to be considered if hydrothermal convection is likely to occur in a sedimentary geothermal reservoir system.

1. INTRODUCTION

Convective heat transfer in sedimentary reservoir systems can significantly increase their geothermal potential, as hot water is transported to shallower depths by zones of upflow (Barbier, 2002). But similarly, the unknown location of such upflow zones increases the exploration uncertainty. Reasons for this are that these zones can be difficult to locate due to uncertain reservoir geometry and reservoir properties (Rana et al., 1979; Schilling et al., 2013), or as they are influenced by active exploitation (Grant et al., 1982). However, knowledge about the convection pattern is important for the success of geothermal projects, as boreholes drilled in a zone of downflow would yield relatively low production temperatures (Fig. 1). As such, knowledge about the state of the convection system and its pattern is crucial for assessing the uncertainty and associated risk of an exploration study. Several parameters, such as aquifer thickness or the magnitude of permeability control whether a heat transport by convection can form. However, as both these parameters vary spatially, using representative averages, e.g. a homogenous permeability, does not provide insight into the spatial distribution of up- and downwelling zones. It is therefore necessary to incorporate more detailed knowledge about these parameters, i.e. their spatial heterogeneity, for predicting the hydrothermal potential of (sedimentary) reservoir systems with convection. While the spatial variation of the reservoir-thickness can be derived from geophysical measurements to quite detail, similarly detailed information about the spatial distribution of permeability is often not available, or difficult to assess, as permeability of sedimentary reservoir systems correlates to the depositional paleo-environment.

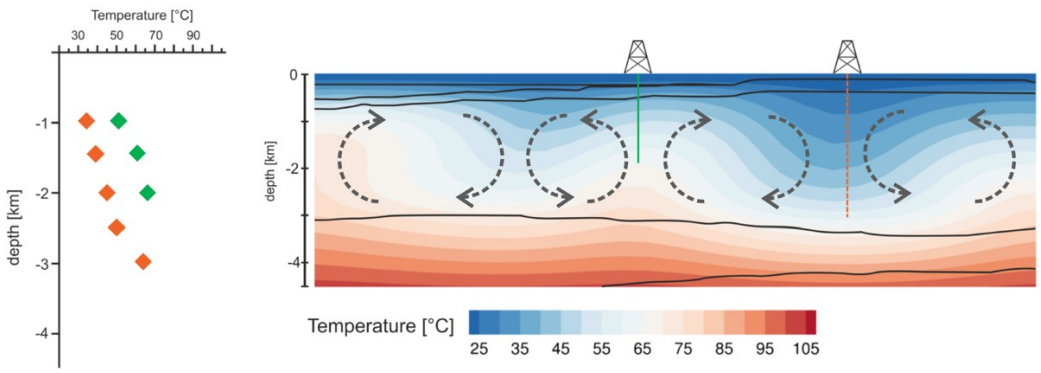


Figure 1: Example how convection in a geothermal reservoir body can influence temperatures in boreholes. Here, drilling in a zone of upflow yields the same temperatures as a borehole 1.5 km deeper (if drilled in a zone of downflow).

Depositional structures may be inferable from seismic sections to some extent (e.g. Back et al., 2011), and seismic properties of rocks can be related to their hydraulic properties (Rubin et al., 1992). But even if such methods are successful, an uncertainty in spatial permeability distribution remains.

One sedimentary reservoir system which probably shows convection is the Perth Basin, a sedimentary rift basin in Western Australia. It extensively studied for its geothermal potential with focus on one prominent reservoir unit, the Yarragadee Aquifer, and multiple modeling studies suggest that hydrothermal convection occurs within the Yarragadee Aquifer (Sheldon et al., 2012; Schilling et al., 2013; Irvine et al., 2015; Niederau et al., 2017). Timms et al. (2015) classified available core material from wells in several lithostratigraphic units corresponding to different depositional paleoenvironments in the Perth Basin. While they found a general correlation between lithostratigraphy and average permeability, the spatial correlation of permeability in the Yarragadee Aquifer remains uncertain. However, for characterizing the convection pattern, knowledge about heterogeneity of permeability and its spatial continuity is crucial, as both influence the convection system in an aquifer (Nield & Simmons, 2007; Nield et al., 2009).

Irvine et al. (2014) created Rayleigh Number maps of the Yarragadee Aquifer, and addressed vertical heterogeneity of permeability in the Yarragadee Aquifer by stratigraphic forward modelling. From the resulting layer-cake model with laterally continuous permeability, they concluded that convection is likely in the Yarragadee Aquifer and that these maps are a suitable tool for locating free convection in the aquifer. Laterally continuous permeability facilitates a characterization based on the Rayleigh Number. However, permeability in aquifers is often laterally discontinuous, and performing a standard Rayleigh number analysis in such heterogeneous porous media is difficult and not straightforward (Nield & Simmons, 2007; Nield et al., 2009). We present a different, thermodynamically motivated measure for characterizing the state of a convection system; the so-called entropy production (Kleidon & Lorenz, 2005; Siavashi et al., 2015; Börsing et al., 2017). While the porous Rayleigh Number is a sound and tested indicator for characterizing a convective system in an aquifer, it needs the two parameters of the porous medium, L (thickness of the porous medium), and $\hat{k}$ (the average permeability). These are not constant in real-world reservoir systems, and usually averaged, i.e. simplified. By assessing the additional heat transport introduced by convection, the measure of entropy production bypasses these two simplifications. Also, a Rayleigh number is a predictive measure of a system, while entropy production is a diagnostic one, thus corresponding closer to the Nusselt number.

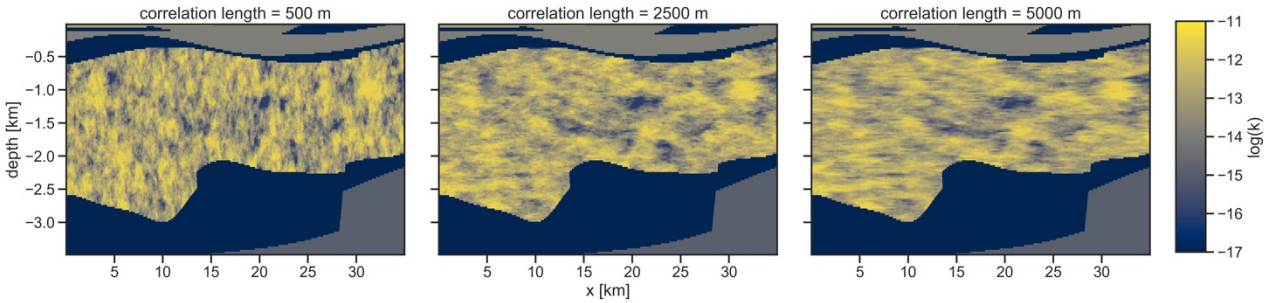


Figure 2: Comparison of three permeability fields in the reservoir model (see Fig. 3) used in this study, only differing in their horizontal correlation length. All three permeability fields are generated from the same random number seed, so the general spatial location of high- and low-permeable areas is preserved. Note that the model is strongly vertically exaggerated.

In this manuscript, we estimate the influence of laterally discontinuous permeability on the associated convection pattern, by systematically increasing the lateral correlation length of porosity and permeability in between ensembles of a 2D cross-section of the Perth Basin model by Niederau et al. (2017). Each ensemble consists of 240 members with equally probable porosity-and permeability fields (e.g. Fig. 2). In order to retain comparability, all ensembles have the same random number seeds.

2. GEOLOGICAL MODEL

The geological model is a 2D section extracted from a 3D geological model of the central Perth Basin presented in Niederau et al. (2017). Its location is indicated by the dashed line in Figure 3. The Perth Basin formed due to rifting between Australia and Greater India in the late Paleozoic to Mesozoic (Harris, 1994), during the breakup of Gondwana. Series of sedimentary rocks filling the Perth Basin can be up to 15 km thick. In the central Perth Basin, thickness of the Yarragadee aquifer ranges from 500 m to about 3000 m. More detailed information about the geological and tectonic history of the Perth Basin can be found in Playford et al. (1976); Backhouse (1984); Harris (1994); Crostella & Backhouse (2000). Lithological units in the geological model are divided depending on their hydraulic properties (see Niederau et al. (2017)), i.e. divided into aquifer and aquitard units, based on geological and petrophysical data (Crostella & Backhouse (2000), Davidson & Yu (2008), Sheldon et al. (2012), Timms et al. (2015)). This is often referred to as “zonation method” (Testerman, 1962; Alpay, 1972). The main aquifer unit of interest is the jurassic Yarragadee Aquifer, which comprises lithologies of three stratigraphical units, namely Cadda-, Yarragadee-, and Gage-formations. Working groups of the Western Australian Geothermal Centre of Excellence (WAGCoE) published several detailed studies covering the petrography of the Yarragadee Aquifer (see Timms et al. (2015) and references therein), its estimated lateral extension and thickness, and estimated temperatures in the aquifer (see Sheldon et al. (2012) and references therein). Our 2D geological model comprises six geological units, (three aquifer units and three aquitard units), dissected by 3 major faults. One fault, the Darling Fault, displaces the sedimentary units of the Perth Basin against the Yilgarn Craton, which bounds the Perth Basin to the East. The Darling Fault is the east boundary of the 2D geological model. Two further faults displace the Basement and the Yarragadee aquifer, visible in the cross-section in Figure3. The Yarragadee Aquifer is covered by Post-rift sediments, of which the South-Perth-Shale acts as a thermal blanket for the Yarragadee Aquifer. In Niederau et al. (2017) we showed that reservoir structure has a potentially stronger impact on a convection pattern compared to spatially heterogeneous permeability. There, we conclude that abrupt changes in reservoir thicknes particularly impact a convective pattern. Consequently, when studying convection in the Perth Basin, fault displacements should be represented

in the model-geometry. The two fault displacements considered in in this study, are at x ≈ 30000 km, and, more pronounced, in the west, at x ≈ 14000 km in Fig.3.

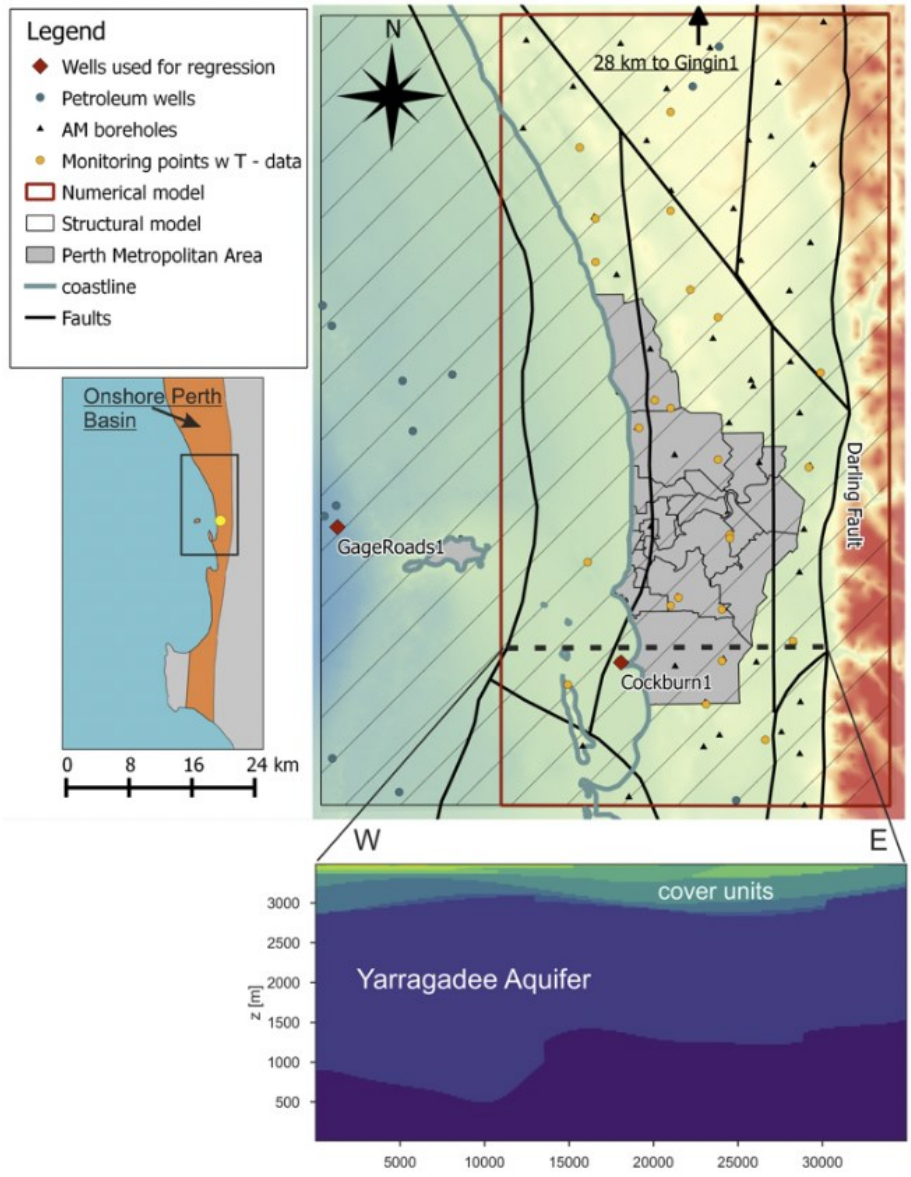


Figure 3: Map showing well locations and model boundaries in the study area in the central Perth Basin (modified from Niederau et al. (2017)). Location of the 2D cross-section is indicated by the dashed line.

However, Niederau et al. (2017) kept the spatial correlation length of permeability constant, thus their conclusion relies on a Monte Carlo study with a singular spatial correlation length. Next to differences in aquifer thickness due to tectonic activity, spatially heterogeneous permeability caused by differential sedimentation and compaction were found to affect a convective pattern. In the following, we will briefly describe the underlying stratigraphic model of the Yarragadee Aquifer, giving insight in the spatial distribution of lithofacies and corresponding spatial differences in aquifer permeability.

2.1 Stratigraphic Model

The Yarragadee Formation was deposited under a predominantly fluvial, more precisely braided river environment, as firstly inferred by Playford et al. (1976) and outlined in more detail in Timms et al. (2015). They classified different lithofacies from multiply wells in the Perth Basin. These lithofacies are irregularly distributed, as they are the direct result of fluvial sedimentation processes, which change with time. In addition to lithofacies classification, Timms et al. (2015) state that porosity strongly correlates with lithofacies in the Yarragadee aquifer, supporting results from earlier studies (Delle Piane et al., 2013). Niederau et al. (2017) used a porosity-permeability relationship based on a fractal pigeon-hole model (Pape et al., 1999), and calibrated it to the Yarragadee aquifer. With lithofacies correlating to porosity and porosity to permeability, permeability can be linked to lithofaces in the Yarragadee aquifer. That is, by varying porosity and permeability spatially, we honor the spatial variability in lithofacies, which was observed by Timms et al. (2015).

2.2 Relating Porosity and Permeability

In the following, we shortly present the histograms for porosity and permeability which are used in a Sequential Gaussian Simulation (Deutsch and Journel, 1998) for generating spatially heterogeneous porosity- and permeability-fields in the Yarragadee Aquifer.

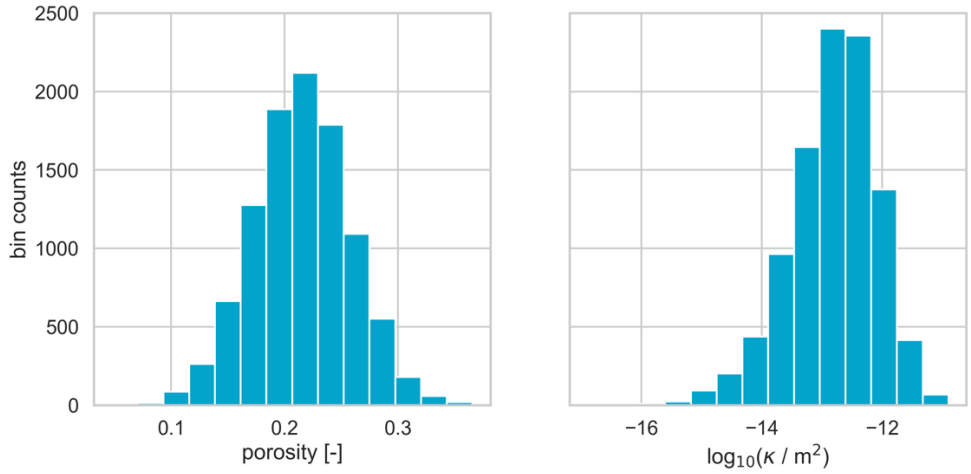


Figure 4: Histograms of porosity and permeability samples used for populating the parameter space in the simulation ensembles. Mean and standard deviation of porosity was deduced by log analysis of the borehole Cockburn 1 (see location in Figure 3). The permeability distribution was calculated from the porosity distribution by applying equation (1).

The aforementioned, relation between porosity and permeability was calibrated to the Yarragadee aquifer based on well data from CSIRO (2007)

$$k = [166\,\phi + 19904\,\phi^{2.8} + 388\,(10\,\phi)^{8.01}] \times 10^{-18} \qquad (1)$$

Where k is permeability in m², and ϕ is porosity. Figure 4 shows multiple porosity samples which are based on mean and standard deviation from a porosity log deduced from the well Cockburn 1. Using equation 1, the according permeability samples (Figure 4 right) were calculated.

3. NUMERICAL MODEL

Based on the 2D geological model geometry presented in Figure 3, we set up a numerical model as the basis for multiple Monte Carlo ensembles for studying the influence of spatial correlation length of permeability on the convection system. Figure 5 shows the model domain colored by the initial temperature field. All parameter values presented in Figure 5 are the same for all Monte Carlo realizations. The only thing which changes, is the spatial continuity of porosity and permeability (see, for instance, Figure 2).

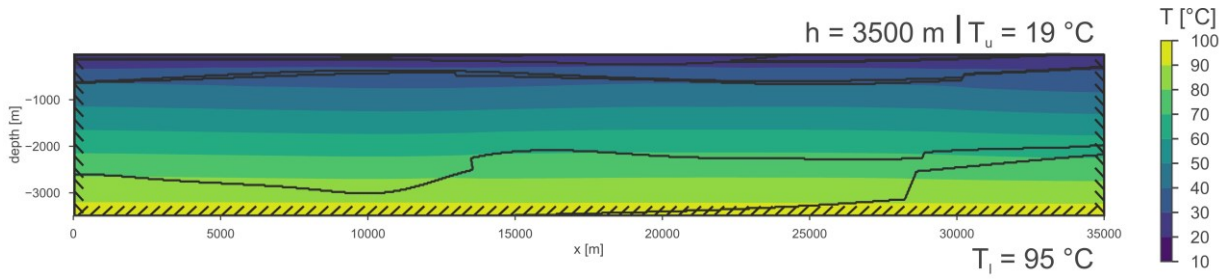


Figure 5: Initial temperature (color coded) and boundary conditions for the 2D model of the Perth Basin. Black lines indicate interfaces between different model units.

Boundary conditions for temperature were set as Dirichlet boundary conditions, i.e. constant temperatures of 19 °C (top boundary) at the surface and 95 °C (bottom boundary) at 3.5 km depth, which is representative for the Perth Basin at these depths (Sheldon et al., 2012; Schilling et al., 2013). The hydraulic potential is set to 3.5 km, implying hydrostatic conditions in the model. As for the top boundary for the hydraulic potential, it was set as a function of topography and sea-level respectively. As no strong topographic increase from sea-level occurs in the onshore part of the model, the top boundary condition varies around 3500 m.

Table 1 lists the main relevant properties for the lithological units incorporated in this model. These values are compiled from multiple literature sources. For the Yarragadee aquifer, Mean represents values used in a comparison simulation with homogeneous porosity and permeability, while Range states the parameter value range bounding the parameters in the heterogeneous scenarios. For determining, when a convection system usually stabilizes in our models, we ran multiple test simulations. These showed that most instabilities occur at short horizontal correlation lengths, but all models showed a stabilized convection system after 60 000 years. Thus, we set the maximal simulation time for the transient models to 60 000 years.

Table 1: Geological units implemented in the 2D model and corresponding petrophysical properties which were used in the simulation. References: (1) CSIRO (2007); (2) Schilling et al. (2013); (3) HDRPL (2008); (4) Botman (2010); (5) Middleton (2013).

Model Unit	Porosity	vertical Permeability	Thermal Conductivity	Radiogenic Heat Production
		(10^{-15} m^2)	(matrix; W m^{-1} K^{-1})	(μW m^{-3})
Leedervilee Aquifer	0.3	1.1810^{-13}	3.4	0.6
South Perth Shale	0.1	0.01	1.8	0.82
Yarragadee Aquifer	Mean: 0.2	Mean: 11.8	4.3	0.52
	Range: 0.14 - 0.33	Range: 0.3 - 4100	4.3	0.52
Cattamarra Coal Measures	0.1	0.018	4.1	0.45
Basement / Yilgarn Craton	0.06	1.1810^{-19}	4	4
References	1	2	3	4,5

3.1 Monte Carlo Ensembles

Using Sequential Gaussian Simulation (Deutsch and Journel, 1998), we create multiple ensembles of different horizontal correlation length in porosity and permeability. We increase the horizontal correlation length from 500 m to 10000 m by 500 m steps, yielding 20 ensembles in total. The vertical correlation length is kept constant at 150 m for the whole ensemble suite. Each ensemble comprises 240 ensemble members. This number results from the architecture of the JURECA-HPC cluster (Jülich Supercomputing Centre, 2016), where we ran the simulations, where we used 10 nodes each having 24 available cores. For assessing the influence of vertical correlation length, we run a second experiment with a vertical correlation length of 100 m.

4. METHODS

In this section, we will briefly describe the forward code used to simulate the convection system, and the diagnostic measure of entropy production.

4.1 Forward code

Simulation of the 2D reservoir model are done using SHEMAT-Suite (Rath et al., 2006), a development based on the SHEMAT code (Clauser and Bartels, 2003). The code models heat- and mass-transport in a porous medium, by solving coupled balance equations for energy, mass, and momentum. The transient flow equation is based on Darcy's law and mass conservation:

$$S_s \frac{\partial h}{\partial t} = \nabla \cdot \left[\frac{\rho_f \, g \, \boldsymbol{k}}{\mu_f} \left(\nabla h_0 + \rho_r \, \nabla z \right) \right] + W \tag{2}$$

Where S_s is the specific storage coefficient [m^{-1}], h the hydraulic potential [m], and t is time [s]. ρ_f is the fluid density [kg m^{-3}], g the gravity [m s^{-2}], $\boldsymbol{k}$ the permeability tensor [m^2], μ_f the dynamic viscosity of the Fluid [Pa s], ρ_r is the relative density change compared to atmospheric temperature, z the vertical space coordinate [m], and W a volume source term [s^{-1}]. Analogue, the heat transport equation is derived from Fourier's law of heat conduction and energy conservation:

$$(\rho c_p)_B \frac{\partial T}{\partial t} = \nabla \cdot \left[(\lambda_B \, \nabla T) - (\rho c_p)_f \boldsymbol{v} \, T \right] + K \tag{3}$$

Where (ρc_p) are the thermal capacities of the *bulk* and *fluid* phase respectively [J m^{-3} K^{-1}], T is Temperature [°C], λ_B is the *bulk* thermal conductivity [W m^{-1} K^{-1}], $\boldsymbol{v}$ the Darcy velocity [m s^{-1}], and K the radiogenic heat production [W m^{-3}]. Values for the bulk porous rock parameters are calculated using the appropriate mixing laws, e.g. geometric mean for the thermal conductivity.

4.2 Entropy Production Number

We will just present the equation for the final entropy production number here. A full and detailed description of the concept of entropy production and derivation of the entropy production number can be found in Börsing et al. (2017). The irreversible production of entropy is caused by thermal- and viscous dissipation. However, considering realistic ranges for the Darcy velocity in an aquifer (10^{-6} m s^{-1} to 10^{-4} m s^{-1}) and the water viscosity, the contribution of viscous dissipation is negligible to the total entropy production for laminar flow in porous media. The entropy production number is a non-dimensionalized form of the total entropy production (Siavashi et al., 2015; Siavashi et al., 2017):

$$N_{\dot{S}} = \frac{\dot{S}_{total}}{VY} \qquad with \qquad Y = \frac{q^2}{\lambda_B T_0^2} \tag{4}$$

Where $N_{\dot{S}}$ is the entropy production number [-], $\dot{S}_{total}$ the total entropy production, V the volume of the model domain [m^3], q the total specific heat flow [W m^{-2}], and T_0 the average initial temperature [°C]. For a conductive case as in Figure 5, T_0 can be averaged by the arithmetic mean between upper and lower temperature boundaries.

5. RESULTS

In this section, we present the simulation results of the aforementioned Monte Carlo ensembles with focus on the influence of changing spatial correlation length, analyzed using the average entropy production number (eq.(4)). Per definition, higher entropy production numbers correspond to more vigorous free convection, i.e. stronger lateral heat transport.

5.1 Average Entropy Production Number with Increasing Horizontal Correlation Length

Figure 6 shows the ensemble average of the entropy production number for increasing finite horizontal correlation lengths from 500 m to 10 000 m. An almost linear decrease of the entropy production number with increasing horizontal correlation length can be observed in the left plot for the interval between 500 m and 6000 m horizontal correlation length. This trend flattens for larger correlation lengths up to 10 000 m. This is due to an increasing number of ensemble members which do not show convection, thus the ensemble average for the entropy production number decreases, as conductive simulations will yield a value for N_S of about 1. However, if we exclude all ensemble members which do not show active convection, the decrease in entropy ceases at a correlation length of about 2000 m. At larger correlation lengths, the average entropy production number stays about constant, suggesting that the convective systems associated to the respective correlation lengths do not differ significantly. For comparison, we plot the entropy production number of a model with homogeneous porosity and permeability. Its entropy production value fits the trend of the decreasing ensemble means.

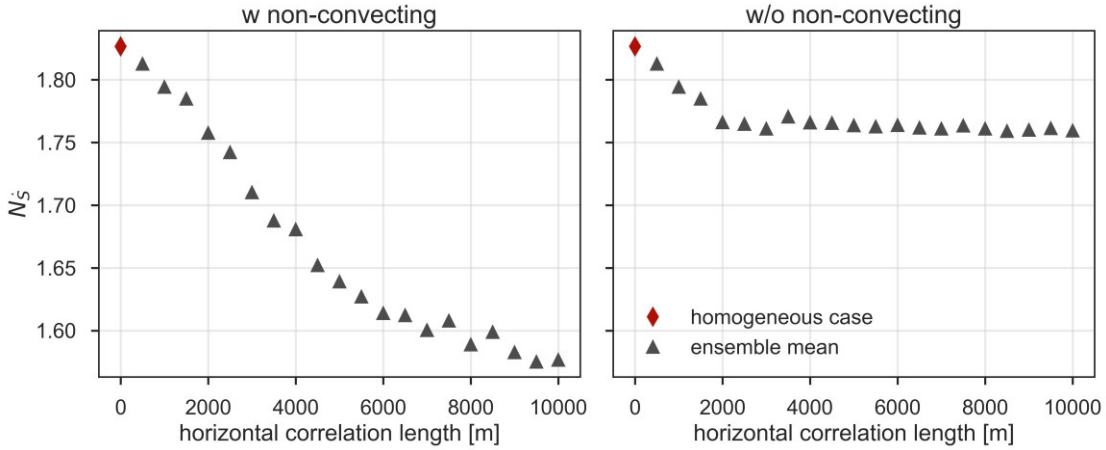


Figure 6: Variation of the ensemble-average entropy production number N_S with different horizontal correlation length (vertical correlation length cl_v = 150m). Left: including non-convecting ensemble members. Right: excluding non-convecting ensemble members.

However, to support this conclusion, we have to analyze the variance of the ensembles with convection. For this, we plot the ensembles (only including members with convection) as boxplots in Figure 7. Similarly to Figure 6 right, the ensembles stabilize at correlation lengths of around 2000 m. The changing whisker-lengths of the boxplots shows however, that no distinct trend in ensemble spread is visible. A similar observation can be made from the changing box-heights.

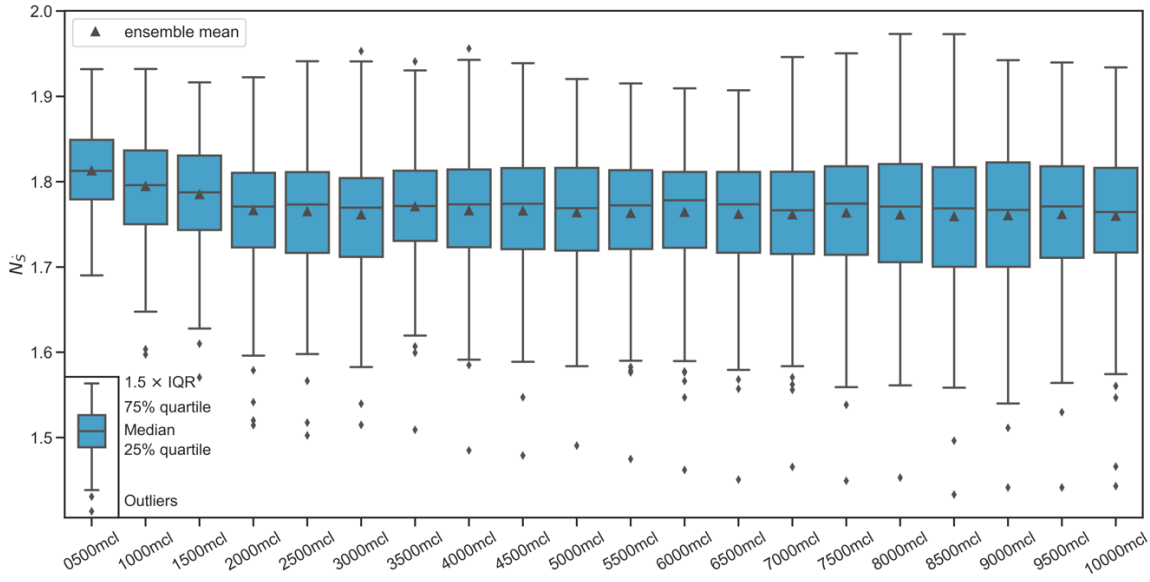


Figure 7: Boxplots of the entropy production number for each ensemble with increasing horizontal correlation length cl_h. As in the mean observation, the average entropy production decreases with increasing cl_h, but stabilises at larger cl_h. IQR stands for inter quartile range (75 % quartile – 25 % quartile).

Outliers (black diamonds) appear to be mainly at lower entropy production numbers. This can be explained by the choice of boundary conditions, which prescribe a strict upper limit for the heat transport in the model, thus limiting the entropy production.

5.2 Influence of Vertical Correlation Length

For assessing the influence of vertical versus horizontal correlation length, we simulated a similar ensemble suite with a fixed vertical correlation length of 100 m. As in the previous part with 150 m vertical correlation length (cl_v), increasing the horizontal correlation length (cl_h) correlates with a decrease in the ensemble mean, i.e. number of ensemble members which show convection. However, the fraction of ensemble members which do not show convection is significantly higher for the experiment with cl_v = 100 m. While over 80% of members in ensembles with cl_v = 150 m show convection, this fraction decreases drastically for ensembles with clv = 100 m down to < 50% (Figure 8).

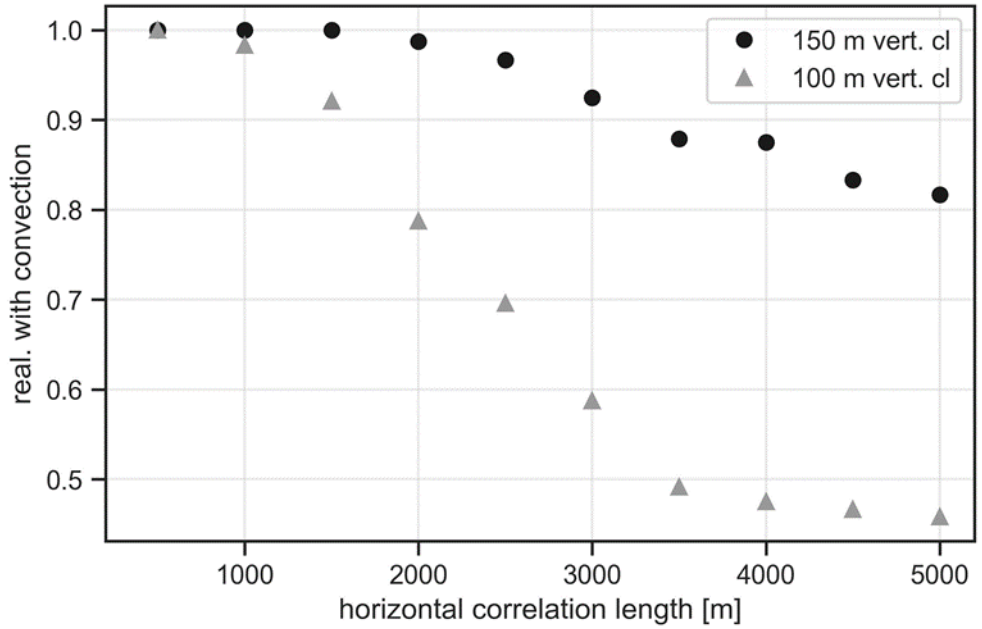


Figure 8: Variation of the fraction of realisations with free convection $N_{convection}$ with horizontal correlation length cl_h for two different cl_v. Ensembles with cl_v = 100 m show a significantly stronger decrease in convecting realisations, compared to ensembles with cl_v = 150 m.

These results emphasize how important knowledge about the (vertical) spatial continuity of permeability in a modeled aquifer is for quantifying the probability of convective heat transport. Further, we observe that cl_v has a stronger influence on the development of convection cells than cl_h, which does not influence the heat transfer, expressed by entropy production over a certain horizontal correlation length. This observation has important implications, as the vertical correlation length clv can usually be deduced from well logs.

DISCUSSION AND CONCLUSION

The numerical experiments were conducted following the hypothesis that the formation of convection systems strongly depends on aquifer heterogeneity and that the horizontal correlation length of reservoir parameters is one controlling factor. Further, it was hypothesized that this influence can be expressed by the entropy production number. The latter is clearly shown, as the entropy production number is sensitive to the number of non-convecting ensemble members, as these yield a low entropy production number of around one.

A model with homogeneous permeability can be treated as a case with an infinite spatial correlation length. In such a model, only the magnitude of permeability determines if convection is likely or not. If we consider the same model with heterogeneous permeability, i.e. a finite correlation length, the magnitude of permeability and its spatial variation would control the onset of free convection. It may appear logical that longer correlation lengths might facilitate the onset of convection, as permeable areas stretch over a longer distance. However, so do areas of low permeability. These work as barriers to the buoyancy-driven convective current, which is mainly vertical. At shorter finite horizontal correlation lenghts, these currents just get diverted around lenses of low permeability, whereas a lateral elongation of those lenses can completely inhibit the onset of convection. And such a lateral elongation corresponds to a longer horizontal correlation length.

Usually thermal Neumann boundary conditions are applied as bottom boundary condition for geothermal reservoir models (e.g. Smith and Chapman, 1983). In the Perth Basin region, several studies use a basal Dirichlet boundary condition for temperature and yield realistic simulation results (Corbel et al., 2012b; Schilling et al., 2013; Niederau et al., 2017). Their results suggest that, for the bottom boundary, a Dirichlet boundary condition for temperature is suitable for the Perth Basin.

A classic approach in studying convecting system is by assessing the systems Rayleigh number. While the Rayleigh number is very useful for estimating if a system is likely to show convection, it does not include information about the likely convective pattern.

The same Rayleigh number may characterize different convection patterns which have different entropy production numbers (Börsing et al., 2017). Also, assessing a meaningful Rayleigh number in a non-idealized setting (e.g. a convecting layer with non-parallel boundaries) is difficult, as the height of the convecting layer, or the temperature difference across it are two input parameters in classical Rayleigh number formulations. Both parameters are not constant in a real-world example.

The measure of entropy production shows to be a powerful diagnostic tool when studying hydrothermal convection in real-world reservoir systems, and that in such settings, it can be more useful than a classical Rayleigh number assessment. It is not fully clear which conditions in our simulations facilitate the development of a convective system. It is likely that certain combinations between heterogeneous permeability and reservoir structure is an important factor for convection in our model of the Perth Basin. Further, our results emphasize that consideration of vertical correlation length is important, as its influence on the formation of a convection system seems stronger than the impact of horizontal correlation length. This is an important finding, as vertical correlation lengths of parameters can be deduced from borehole logs.

ACKNOWLEDGEMENTS

The authors gratefully acknowledge the computing time granted by the JARA-HPC Vergabegremium on the supercomputer JURECA at Forschungszentrum Jülich for the JARA-HPC project 11061.

REFERENCES

Alpay, O. A.: A practical approach to defining reservoir heterogeneity. Journal of Petroleum Technology, **24**(07), (1972), 841-848.

Back, S., Van Gent, H., Reuning, L., Grötsch, J., Niederau, J., and Kukla, P.: 3D seismic geomorphology and sedimentology of the Chalk Group, southern Danish North Sea. Journal of the Geological Society, **168**(2), (2011), 393-406.

Backhouse, J.: Revised late Jurassic and early Cretaceous stratigraphy in the Perth Basin, Geological Survey of Western Australia Report, **12**, (1984), 1–6.

Barbier, E.: Geothermal energy technology and current status: an overview, Renewable and Sustainable Energy Reviews, **6**(1), (2002), 3–65.

Botman, C.: Determining the geothermal properties of the perth basin lithology to aid geothermal energy projects, Perth: Curtin University of Technology. B. Sc.(Geophysics) Honours thesis, unpublished, (2010).

Börsing, N., Wellmann, J. F., Niederau, J., and Regenauer-Lieb, K.: Entropy production in a box: Analysis of instabilities in confined hydrothermal systems, Water Resources Research, **53**(9), (2017), 7716–7739.

Crostella, A. and Backhouse, J. Geology and petroleum exploration of the central and southern Perth Basin, Western Australia, **57**, (2000), Geological Survey of Western Australia

CSIRO: Csiro Pressureplot(tm) software and Pressuredb (tm) database, www.pressureplot.com, (2007).

Davidson, W. A. and Yu, X.: Perth regional aquifer modelling system (PRAMS) model development: Hydrogeology and groundwater modelling, Western Australia Department of Water, Hydrogeological record series HG20, (2008).

Delle Piane, C., Esteban, L., Timms, L., & Ramesh Israni, S.: Physical properties of mesozoic sedimentary rocks from the perth basin, western australia, Australian Journal of Earth Sciences, **60**(6-7), (2013), 735–745.

Deutsch, C. and Journel, A.: GSLIB Geostatistical software library and user's guide, Oxford University Press, New York, (1998).

Grant, M., Donaldson, I., and Bixley, P.: Geothermal reservoir engineering, Academic Press, New York, (1982).

Harris, L.: Structural and tectonic synthesis for the perth basin, western australia, Journal of Petroleum Geology, **17**(2), (1994), 129–156.

HDRPL: Geothermal energy potential in selected areas of Western Australia (Perth Basin), Hot Dry Rocks Pty Ltd. (HDRPL), South Yarra, Australia, (2008).

Irvine, D. J., Sheldon, H. A., Simmons, C. T., Werner, A. D., and Griffiths, C. M.: Investigating the influence of aquifer heterogeneity on the potential for thermal free convection in the Yarragadee Aquifer, Western Australia. Hydrogeology Journal, **23**(1), (2015), 161-173.

Jülich Supercomputing Centre, 2016. Jureca: General-purpose supercomputer at ju¨lich supercomputing centre, Journal of large-scale research facilities, 2(A62).

Kleidon, A. and Lorenz, R.: Entropy production by earth system processes, in A. Kleidon & R. Lorenz (eds.), Non-equilibrium Thermodynamics and the Production of Entropy, (2005), pp. 1–20, Springer, Heidelberg.

Niederau, J., Ebigbo, A., Marquart, G., Arnold, J., and Clauser, C.: On the impact of spatially heterogenous permeability on free convection in the Perth Basin, Australia, Geothermics, **66**, (2017), 119–133.

Nield, D. and Simmons, C. T.: A discussion on the effect of heterogeneity on the onset of convection in a porous medium, Transport in porous media, **68**(3), (2007), 413–421.

Nield, D., Kuznetsov, A., and Simmons, C. T.: The effect of strong heterogeneity on the onset of convection in a porous medium, Transport in porous media, **77**(2), (2009), 169.

Nield, D., Kuznetsov, A., and Simmons, C. T.: The effect of strong heterogeneity on the onset of convection in a porous medium: 2d/3d localization and spatially correlated random permeability fields, Transport in porous media, **83**(3), (2010), 465–477.

Pape, H., Clauser, C., and Iffland, J.: Permeability prediction based on fractal pore-space geometry. Geophysics, **64**(5), (1999), 1447-1460.

Playford, P. E., Cockbain, A. E., and Low, G.: Geology of the Perth Basin, Western Australia, (1976), Geological Survey of Western Australia, Perth, Australia.

Rana, R., Horne, R., and Cheng, P.: Natural convection in a multi-layered geothermal reservoir, Journal of Heat Transfer, **101**(3), (1979), 411–416.

Rubin, Y., Mavko, G., and Harris, J.: Mapping permeability in heterogeneous aquifers using hydrologic and seismic data, Water Resources Research, **28**(7), (1992), 1809– 1816.

Schilling, O., Sheldon, H., Reid, L., and Corbel, S.: Hydrothermal models of the perth metropolitan area, western australia: implications for geothermal energy, Hydrogeology Journal, **21**(3), (2013), 605–621.

Sheldon, H. A., Florio, B., Trefry, M. G., Reid, L. B., Ricard, L. P., and Ghori, K. A. R.: The potential for convection and implications for geothermal energy in the perth basin, western australia, Hydrogeology Journal, **20**(7), (2012), 1251–1268.

Siavashi, M., Bahrami, H. R. T., and Saffari, H.: Numerical investigation of flow characteristics, heat transfer and entropy generation of nanofluid flow inside an annular pipe partially or completely filled with porous media using two-phase mixture model, Energy, **93**, (2015), 2451–2466.

Siavashi, M., Bordbar, V., and Rahnama, P.: Heat transfer and entropy generation study of non-Darcy double-diffusive natural convection in inclined porous enclosures with different source configurations. Applied thermal engineering, 110, (2017), 1462-1475.

Smith, L. and Chapman, D. S.: On the thermal effects of groundwater flow: 1. regional scale systems, Journal of Geophysical Research: Solid Earth (1978–2012), **88**(B1), (1983), 593–608.

Testerman, J.: A statistical reservoir-zonation technique, Journal of Petroleum Technology, **14**(08), (1962), 889–893.

Timms, N. E., Olierook, H. K., Wilson, M. E., Delle Piane, C., Hamilton, P. J., Cope, P., and Stütenbecker, L.: Sedimentary facies analysis, mineralogy and diagenesis of the mesozoic aquifers of the central perth basin, western australia, Marine and Petroleum Geology, **60**, (2015), 54–78.